Macromolecules
COMMUNICATION TO THE EDITOR

Macromolecules **2009**, *42*, 7623–7626 **7623**
DOI: 10.1021/ma901543c

Criteria of Process Optimization in Binary Polymer Blends with Both Phase Separation and Crystallization

Yanhua Niu,[†] Liang Yang,[†,‡] Howard Wang,[§] and Zhigang Wang*,[†]

[†]*CAS Key Laboratory of Engineering Plastics, Beijing National Laboratory for Molecular Sciences, Institute of Chemistry, Chinese Academy of Sciences, Beijing 100190, P. R. China,* [‡]*Graduate School, Chinese Academy of Sciences, Beijing 100049, P. R. China, and* [§]*Department of Mechanical Engineering and Institute for Materials Research, Binghamton University, Binghamton, New York 13902*

Received July 15, 2009
Revised Manuscript Received September 27, 2009

Blending is an important technology and often used in manufacturing plastic products to meet design requirements at a low cost. In cases where mechanical properties are of the primary concern, a more expensive high performance polymer is often mixed with a low performance but cheaper polymer to balance the performance, the processability, and the cost. Because polymers are often immiscible with each other and are used in the semicrystalline state, the morphology of polymer blends (therefore their properties and performance) is largely determined by the interplay between liquid−liquid phase separation (LLPS) and crystallization. This complication in many cases limits the control of properties of the final products, whereas in other cases, morphologies arising from the interplay between transitions could lead to new structures and dynamics and result in superior or novel products.[1−3] A fundamental understanding of the LLPS/crystallization coexistence is the key for improving many commodity products, such as automotive bumpers, and for developing novel applications, such as membranes and scaffolds in biotechnology.

In a binary polymer blend with one crystallizable component, intertwined complex phase and crystalline morphologies with multiple length scales can be created depending on processing conditions,[4,5] which tune the competitions among thermodynamic driving forces and interplays among several kinetic-controlled processes. For example, previous studies have shown that LLPS or, specifically, spinodal decomposition in near-critical polymer blends precedes and then accelerates crystallization,[6−9] which is attributed to a fluctuation-assisted crystallization mechanism.[10−13]

For structural materials applications, morphologies of polymer blends resulting from the dynamic interplay between LLPS and crystallization are necessarily related to their mechanical properties. Several recent studies have shown profound effects of sequential LLPS and crystallization on mechanical properties of polyolefin blends,[14,15] whereas the consequences of more industrial-relevant processes of simultaneously occurring LLPS and crystallization remain illusive. *In situ* rheological monitoring of the phase transformation processes could be a particularly powerful tool for understanding the structure development[16−22] and eventual process optimization. In this Communication, we discuss the criteria of process optimization based on the *in situ* storage modulus measurement during simultaneous LLPS and crystallization in a model polyolefin blend.

*Corresponding author: Tel 011-86-10-62558172; Fax 011-86-10-62558172; e-mail zgwang@iccas.ac.cn.

The polymers used in this study are statistical copolymers of poly(ethylene-*ran*-hexene) (PEH, M_w = 112 000 g/mol, $M_w/M_n \sim 2$, mass density of 0.922 g/cm^3, and branch density of 9-C_4H_9 units per 1000 backbone carbons) and poly(ethylene-*ran*-butene) (PEB, M_w = 70 000 g/mol, $M_w/M_n \sim 2$, mass density of 0.875 g/cm^3, and branch density of 77-C_2H_5 units per 1000 backbone carbons), synthesized using metallocene catalysts. The melting points T_m of PEH and PEB were 119.8 and 48.6 °C, respectively, determined by DSC measurements at a heating rate of 10 °C /min. The phase diagram of PEH/PEB blends has been determined previously,[23] as shown in Figure 1. The LLPS phase boundary possesses an upper critical solution temperature (UCST) behavior at T_c = 146 °C at the critical volume fraction composition, ϕ_c = 0.44, in the melt and follows the Flory−Huggins theory for binary polymer mixtures. The equilibrium melting temperature, $T_m°$, of blends decreases with increasing PEB concentration in the one-phase regime, whereas $T_m°$ remains relatively constant in the two-phase regime, at ca. 127 °C.

Specimens of PEH/PEB blends were prepared by solution coprecipitation[24] to maintain homogeneous compositions in blends, denoted as H20, H30, ..., H80 for 20, 30, ..., 80 wt % PEH in blends, respectively. Blends were melted at 160 °C for 20 min to eliminate the thermal history before quenching to the target temperature at 120 °C for isothermal crystallization. Rheological measurements were carried out using a TA AR2000 stress-controlled rheometer with 25 mm diameter parallel plates. In the oscillatory time sweep measurements, the frequency was fixed at 1 rad/s and the strain at 0.5−1.0%. The normal force control was set to be active to exclude effect of sample shrinkage induced by crystallization. Optical microscopy (OM) studies were carried out on H60 and H70 hot-pressed between two glass plates at 160 °C to form films with thicknesses of ca. 20 μm to avoid overlaps of the crystal nuclei and spherulites. The sandwiched samples were placed in a Linkam-350 hot stage and heated to 160 °C for 10 min followed by quenching to the isothermal temperature of 120 °C. Optical micrographs were recorded *in situ* using a Leica DMLP polarized optical microscope equipped with a Pixera Penguin 150CL CCD camera. All the rheological and OM experiments were conducted in a nitrogen atmosphere.

Figure 2 shows the evolution of storage modulus, G', for pure polymers and PEH/PEB blends at 120 °C. Neat PEB shows a constant G', reflecting an invariant molten state, whereas neat PEH shows that after an initial incubation period, G' increases rapidly and reaches a plateau, displaying characteristics of the isothermal crystallization process. The crossover time from rapid growth (primary crystallization) to plateau (secondary crystallization)[25] is denoted as t_c. Blends show two kinds of behaviors: those with slowly and continuously increasing G' values at low PEH compositions (H20 and H30) and those similar to PEH at higher PEH compositions (H40−H80). It is conceivable that isolated crystallites grow in the former whereas crystals fill up the sample volume in the latter. In typical mixtures, both the magnitude and kinetics of G increase monotonically with the composition of the crystallizable component, whereas the intriguing observation here is that there exist multiple crossovers among H50, H60, and H70 for t = 10−120 min, as shown in Figure 2. The most prominent feature is that G' of H60 increases rapidly to exceed that of H70 and remains higher throughout the rest of the measurement (highlighted by the blue and red symbols). Even H50 briefly exceeds H70 during the observation window of ca. 50−100 min. To ensure that

Published on Web 10/02/2009

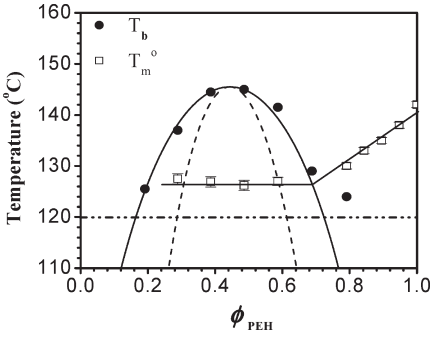

Figure 1. Phase diagram of the PEH/PEB blends. The filled circle indicates binodal temperature T_b (solid line is the fitted curve), and the dashed line indicates spinodal curve. $T_m°$ denotes the equilibrium melting temperature. The selected crystallization temperature of 120 °C is marked by a dash-dot line, at which PEH is crystallizable, while PEB is molten.

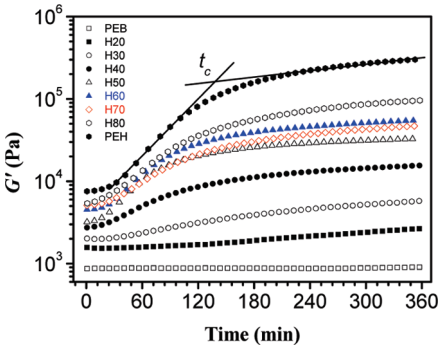

Figure 2. Evolution of storage modulus, G', for pure polymers and PEH/PEB blends at 120 °C. Neat PEB shows a constant G' in the molten state, whereas neat PEH displays characteristics of the isothermal crystallization process. Similar features are found in blends with a PEH composition >30%. The crossover time from rapid growth to plateau is denoted as t_c.

these observations are not experimental artifacts, the entire set of measurements has been carried out at a low frequency, 0.1 rad/s, with otherwise the same conditions. The data show qualitatively the same characteristics; i.e., G' of H60 increases faster and remains higher than that of H70 (see Supporting Information[26]).

According to the phase diagram in Figure 1, H60 and H70 at 120 °C are both in two-phase regimes and below the $T_m°$, so both LLPS and crystallization would occur if a homogeneous mixture is quenched to that temperature. The kinetic interplay between LLPS and crystallization in PEH/PEB blends has been previously studied.[11] Spinodal decomposition always precedes crystallization at the initial stage because an unstable liquid mixture segregates spontaneously, whereas a metastable supercooled liquid solidifies through the nucleation and growth. For the late stage LLPS, phase coarsening is hydrodynamics-driven; experimental data and scaling arguments on critical blends show a crossover temperature at 118 °C, above which liquid phase domains grow faster than crystallites. In this study, the process temperature is at 120 °C, above the crossover temperature but far below the critical temperature. As a result of such deep quench, LLPS is at the late stage throughout the experimental time, ensuring the faster LLPS kinetics in near-critical blends H50 and H60. Note that the above rate comparison is made assuming that LLPS is independent of crystallization. Once the crystallization begins, LLPS is largely inhibited due to the drastically increased viscosity. Although the effect of LLPS is confined to the early times of the process, as will be discussed below, LLPS is important in assisting the nucleation of crystals and defining the overall morphological textures.

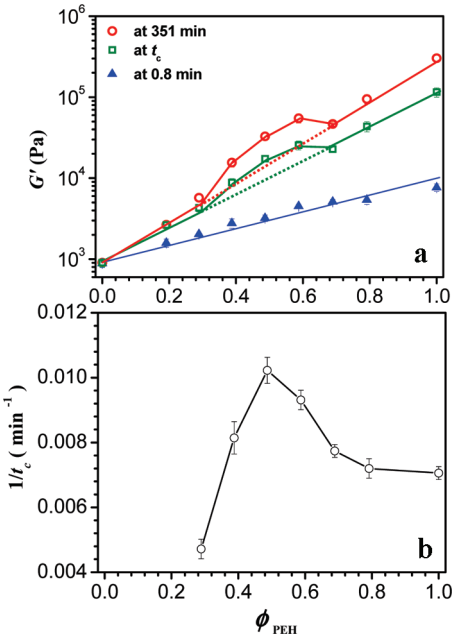

Figure 3. (a) G' values corresponding to the initial molten (at 0.8 min), intermediate crossover (at t_c), and late plateau (at 351 min) states, respectively. (b) Variation of the inverse of the crossover time, $1/t_c$, as a function of the PEH volume fraction.

When H60 is quenched to 120 °C, the mixture is unstable and spontaneous spinodal decomposition occurs, followed by the accelerated nucleation of crystals in the phase separating medium. LLPS-enhanced crystallization has been a topic of recent research interest, with its origin still under debate.[7−10,12,27] A general observation is that nucleation occurs preferentially at the interface of coexisting phases. As large interfacial areas can be generated during spinodal decomposition as in H60, nucleation and growth of phase domains in metastable H70 results in slower creation of interfaces and therefore slower nucleation of crystallites. That explains the faster kinetics of H60. On the other hand, the higher G' of the final products of H60 could be due to the interconnected PEH-rich and PEB-rich phases from LLPS separation, which have a negligible effect on G' in the initial molten state but offer superior spatial distribution as higher G' crystallites form preferentially in the PEH-rich network phase.

To compare the composition dependence of G' at different stages of structural development, Figure 3a shows G' values corresponding to the initial molten (at 0.8 min), intermediate crossover (at t_c), and late plateau (at 351 min) states. In the initial molten state, G' depends almost linearly with PEH composition in a semialgorithmic scale, following the mixing rule of polymer melts.[28] In contrast, the variations of G' at both t_c and 351 min deviate from the simple linear relationship for blends near the critical composition, i.e., H40, H50, and H60. Their G' values are greater than ones following the mixing rule. As discussed above, spinodal decomposition in near-critical blends could result in interconnected bicontinuous morphology, which in turn influences the distribution of subsequently formed crystals to yield more effective structural reinforcement. Because the origin lies in the LLPS structure, the effect is already evident during the primary crystallization stage and persists after much of the secondary crystallization stage.

The influence of LLPS on the rate of crystallization (therefore the increase rate of G') is characterized by the inverse of t_c, as shown in Figure 3b. Except for H30, the rate is higher in blends than in the pure PEH, with the maximum rate at 50% PEH, near the critical composition. As discussed previously, LLPS in blends results in heterogeneous compositions and large interfacial areas

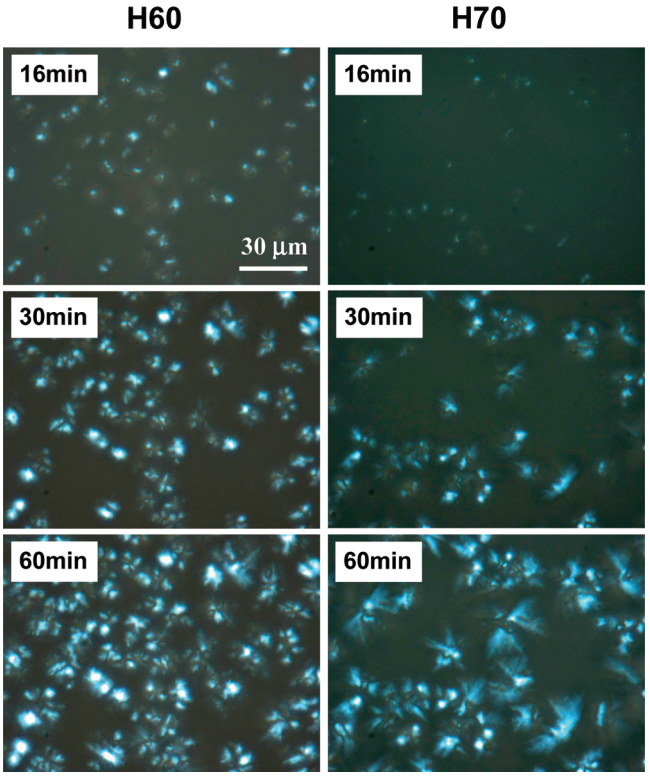

Figure 4. *In situ* polarized optical micrographs of H60 and H70 after various times at 120 °C. Faster nucleation rate and higher crystal density in H60 are evident.

that facilitate the nucleation of crystallites. The effect of phase separation overwhelms the larger undercooling for crystallization in the pure PEH. As LLPS is controlled by the quench depth, the kinetics is the fastest in blends near the critical composition; the same is true for the crystallization kinetics. This is consistent with the polarized OM observation. Figure 4 shows the optical micrographs of H60 and H70 stored at 120 °C for various times. Evidently, after the same isothermal time, the number density of crystals is higher in H60. Furthermore, spinodal decomposition in a binary liquid mixture results in well-defined phase patterns that serve as a template for an even spatial distribution of relatively uniform sized spherulites, consistent with the findings in a recent simulation study of polymer solutions and blends.[27] Such structure is analogous to a reinforcing network of crystallites, resulting in persistently higher G' in H60 than in H70 after the initial nucleation. The micrographs also show that at long isothermal times crystals could grow into PEH-poor phases and fill the volume, consistent with previous experimental observations on this blend[15] and others.[1,5,29] Volume filling by crystals could be advantageous for a larger G'.

On the basis of the above observations, we further discuss the criteria of process optimization in polymer blends with both LLPS and crystallization using a performance-to-cost ratio (PCR) quantity. For structural applications, the performance is a function of G' and other characteristics. For the sake of simplicity and conceptual argument, here we use $\log(G')$ to indicate the performance. The costs of a unit product include materials (M) and processing (P) normalized by throughput, $M + P\tau$, where τ is the time for producing each unit, and is related to human and equipment (capital investment and depreciation) costs. In a typical materials formulation, the cost increases linearly with the composition of more costly and higher performance component, Φ. The processing cost is related to the equipment operation including energy input and other consumables. Energy consumption becomes a more significant factor, which is scaled as a power law of the processing temperature, T^a. So PCR $= \log(G')/[M(\Phi) + T^a\tau]$. In this study, we have shown that at a constant T the presence of LLPS during the blend processing improves PCR in two aspects. (1) In many cases, fulfilling the mixing rule is already much desirable since mixing could also deteriorate the performance of final products; gaining above the mixing rule is a plus. In this work, the superior mechanical property of H60 to that of H70 implies more advantageous of using phase separation to control the morphology. As the contribution toward G' is solely due to PEH crystals, H50 and H60 gain about 35% and 19% in PCR compared with H70, respectively. (2) If processing poses as a large component in the cost structure, the production rate, or the inverse of the processing time, is of primary interest. As shown in Figure 2, t_c is the crossover time separating the fast and slow growth regions of G', it is advantageous processing the polymer using the fast regime to the furthest extent. On the basis of the data in parts a and b of Figure 3, the PCR gains of H50 and H60 are ca. 26% and 19% over H70, respectively. This simple analysis conceptually illustrates the benefit of blending enhanced by LLPS. The assessment of PCR involving the properties of final product and the real manufacturing setting is beyond the scope of this fundamental study.

In this study, we illustrate the enhanced crystallization in the presence of liquid−liquid phase separation in binary polymer blends, resulting in superior mechanical properties. In addition to resulting in the higher crystallization rate and the larger nucleation density, liquid−liquid phase separation generates interconnected biphasic networks that template the formation of crystal network, which is more effective in structure reinforcement than a blend containing 10% more crystallizable component. On the basis of the experimental data, we discuss the criteria of process optimization using a performance-to-cost ratio quantity. It is conceivable that complex interplay between crystallization and liquid−liquid phase separation could offer a large parameter space for materials selection and process control.

Acknowledgment. Y. H. Niu and Z. G. Wang thank the financial support from the National Science Foundation of China under Grant 20674092. Z. G. Wang thanks the financial support from the National Science Foundation of China under Grant 10590355 for the Key Project on Evolution of Structure and Morphology during Polymer Processing. H. Wang thanks the support from the National Science Foundation of USA under Grant DMR-0711013.

Supporting Information Available: Low-frequency measurements of the storage modulus, G', for neat polymers and PEH/PEB blends at 120 °C. This material is available free of charge via the Internet at http://pubs.acs.org.

References and Notes

(1) Tanaka, H.; Nishi, T. *Phys. Rev. Lett.* **1985**, *55*, 1102–1105.
(2) Tanaka, H.; Nishi, T. *Phys. Rev. A* **1989**, *39*, 783–794.
(3) Jungnickel, B.-J. *Lect. Notes Phys.* **2003**, *606*, 208–237.
(4) Inaba, N.; Sato, K.; Suzuki, S.; Hashimoto, T. *Macromolecules* **1986**, *19*, 1690–1695.
(5) Inaba, N.; Yamada, T.; Suzuki, S.; Hashimoto, T. *Macromolecules* **1988**, *21*, 407–414.
(6) Burghardt, W. R. *Macromolecules* **1989**, *22*, 2482–2486.
(7) Tomura, H.; Saito, H.; Inoue, T. *Macromolecules* **1992**, *25*, 1611–1614.
(8) Chen, H. L. *Macromolecules* **1995**, *28*, 2845–2851.
(9) Madbouly, S. A.; Ougizawa, T. *Macromol. Chem. Phys.* **2004**, *205*, 1923–1931.
(10) (a) Zhang, X. H.; Wang, Z. G.; Muthukumar, M.; Han, C. C. *Macromol. Rapid Commun.* **2005**, *26*, 1285–1288. (b) Zhang, X. H.; Wang, Z. G.; Dong, X.; Wang, D. J.; Han, C. C. *J. Chem. Phys.* **2006**, *125*, 024907. (c) Zhang, X. H.; Wang, Z. G.; Zhang, R. Y.; Han, C. C.

Macromolecules **2006**, *39*, 9285–9290. (d) Shimizu, K.; Wang, H.; Matsuba, G.; Wang, Z. G.; Kim, H.; Peng, W. Q.; Han, C. C. *Polymer* **2007**, *48*, 4226–4234.
(11) Wang, H.; Shimizu, K.; Kim, H.; Hobbie, E. K.; Wang, Z. G.; Han, C. C. *J. Chem. Phys.* **2002**, *116*, 7311–7315.
(12) Niu, Y. H.; Wang, Z. G.; Avila Orta, C.; Xu, D. H.; Wang, H.; Shimizu, K.; Hsiao, B. S.; Han, C. C. *Polymer* **2007**, *48*, 6668–6680.
(13) Hong, S.; Zhang, X. H.; Zhang, R. Y.; Wang, L.; Zhao, J.; Han, C. C. *Macromolecules* **2008**, *41*, 2311–2314.
(14) Pang, Y. Y.; Dong, X.; Zhao, Y.; Han, C. C.; Wang, D. J. *Polymer* **2007**, *48*, 6395–6403.
(15) Yang, L.; Niu, Y. H.; Wang, H.; Wang, Z. G. *Polymer* **2009**, *50*, 627–635.
(16) Khanna, Y. P. *Macromolecules* **1993**, *26*, 3639–3643.
(17) Pogodina, N. V.; Winter, H. H. *Macromolecules* **1998**, *31*, 8164–8172.
(18) Horst, R. H.; Winter, H. H. *Macromolecules* **2000**, *33*, 130–136.
(19) Boutahar, K.; Carrot, C.; Guillet, J. *Macromolecules* **1998**, *31*, 1921–1929.
(20) Coppola, S.; Acierno, S.; Grizzuti, N.; Vlassopoulos, D. *Macromolecules* **2006**, *39*, 1507–1514.
(21) Pogodina, N. V.; Jeong, Y. G.; Ramalingam, S.; Jiang, C.; Hsu, S. L.; Paul, C. W. *Macromolecules* **2006**, *39*, 6672–6676.
(22) Jeong, Y. G.; Pagodina, N. V.; Jiang, C.; Hsu, S. L.; Paul, C. W. *Macromolecules* **2006**, *39*, 4907–4913.
(23) Wang, H.; Shimizu, K.; Hobbie, E. K.; Wang, Z. G.; Meredith, J. C.; Karim, A.; Amis, E. J.; Hsiao, B. S.; Hsieh, E. T.; Han, C. C. *Macromolecules* **2002**, *35*, 1072–1078.
(24) Niu, Y. H.; Wang, Z. G. *Macromolecules* **2006**, *39*, 4175–4183.
(25) Marand, H.; Alizadeh, A. *Polym. Mater. Sci. Eng.* **1999**, *81*, 238.
(26) Supporting Information is available online.
(27) (a) Zha, L.; Hu, W. *J. Phys. Chem. B* **2007**, *111*, 11373–11378. (b) Ma, Y.; Zha, L.; Hu, W.; Reiter, G.; Han, C. C. *Phys. Rev. E* **2008**, *77*, 061801.
(28) Utracki, L. A. *Polymer Alloys and Blends*; Hanser Publishers: New York, 1990.
(29) Cham, P. M.; Lee, T. H.; Marand, H. *Macromolecules* **1994**, *27*, 4263–4273.